

How to minimize the impact of solar panels in weak grids

Pedro Paiva
Supervisor: Prof. Rui Castro

Instituto Superior Técnico, Lisboa, Portugal

October 2022

Abstract

It is clear that to achieve an energy sector independent from fossil fuels there must be a considerable increase in the penetration of variable renewable energy sources like solar and wind power. However, these energy sources do not provide inertia to the system (like the conventional thermoelectric power stations), which is essential to maintain the stability of the grid frequency. In this study, a grid with power generation from each source similar to Madeira island was created on the platform Matlab/Simulink. In this grid, it was considered solar, wind, hydro and thermoelectric generation to correctly represent the Madeira island energy panorama. Three different scenarios were considered, one with the current Madeira island power generation, a future scenario with a considerable increase in the percentage of PV generation and the same future scenario but with a battery energy storage system. And then, several studies were performed to verify the impact on the frequency stability of a ground fault and of a rapid load/generation change. The thermoelectric power plant generator desynchronized and the system collapsed in several of the simulations performed in the future scenario. When a battery system was added, a substantial improvement in the frequency stability was verified and the thermoelectric power plant generator could go back to a steady state after every disturbance. Furthermore, the maximum frequency deviation and the absolute value of ROCOF got smaller relatively to the future scenario without a battery system and even related to the current scenario.

Keywords: BESS; weak grid; Madeira island; solar; renewable; PV

PV	photovoltaic
SG	synchronous generator
MPPT	maximum power point tracking
Id	active current
VSC	Voltage Source Converter
BESS	battery energy storage system
vRES	variable renewable energy sources
ROCOF	Rate of Change of Frequency
DFIG	doubly fed induction generator

tric power stations are synchronously connected and have rotating parts which can be used as an energy buffer to deliver inertia to the system. The wind and solar sources are connected by converters so they cannot contribute to the inertia of the system. So an increase in vRES penetration will lead to a decrease in the inertia of the system if no further measures are taken. The decrease of the inertia of the system can lead to deviations from the frequency's nominal value which can have negative implications and even damage grid systems. It is expected that photovoltaic (PV) generation will increase a lot in the following decades considering the decreasing prices, lower environmental impacts, independence on fuel costs, relatively low operations and maintenance requirements and modular design that facilitates rapid construction schedules. Nonetheless, in small isolated grids like islands and some cities in developing countries, the increase in the penetration of solar generation needs to be studied carefully. These weak grids usually already have low system inertia and low network equivalent impedance (i.e., short-circuit capacity). Therefore, increasing the PV penetration may worsen this situation. This work will study the influence of a

1. Introduction

To achieve an energy sector independent from fossil fuels, it is essential to increase the penetration of variable renewable energy sources (vRES) like solar and wind power. This increase in the penetration of vRES creates significant challenges to the stability of the energy system. First, because vRES are very dependent on the meteorological situation and even on the seasons of the year so, by increasing its integration, the power supply starts to be dependent on factors that cannot be controlled. Furthermore, the traditional thermoelec-

battery energy storage system (BESS) on the frequency regulation of a weak grid in a scenario of high penetration of vRES, which do not contribute to the inertia of the system. To do this, Madeira island will be used as a case study and three scenarios will be considered: current scenario (less vRES penetration), future scenario (more vRES integration) and future scenario with BESS. Then, load, generation and ground fault disturbances will be applied to the system and their effect on the frequency stability will be analyzed. Furthermore, the positive influence the BESS can have in minimizing frequency disturbances will also be studied. The package Simscape Electrical from Matlab/Simulink will be used to perform this study. This report is divided into six parts. Chapter 1 introduces the problem of low inertia in weak grids with large vRES integration and the objectives of the study that will be performed. A brief description of the study itself is also presented. In chapter 2 it is made a case study (Madeira island) characterization and the scenarios definition. Then, it is explained how the simulations will be performed and the disturbances that will be applied. In chapter 3, the grid modeling is explained, describing how each grid element was modelled. In chapter 4, the results are presented and discussed and the conclusion is presented in chapter 5.

2. Simulation Conditions

2.1. Characterization of the power system of the Madeira island

To perform a study on the impact in the frequency of a more considerable PV penetration and an ancillary BESS in the Madeira island is essential to characterize this island. The impact of a bigger PV and of the addition of a BESS will be studied by analyzing the transient state (after load/generation/ground fault disturbances). For that, it is essential to have data about Madeira island that serves as a case study.

The Madeira electrical system comprises thermal, hydro, solid-waste, wind and solar generation units. Furthermore, the penetration of renewable energy sources will increase in the following years, namely by introducing a BESS of 15 MW of power and 10 MWh of storage. The Madeira island has a total installed power of 374.24 MW.

For this study, it will be considered the data included in the 2020 report "Caracterização da rede de transporte e distribuição em AT e MT" made by the EEM (Empresa de Electricidade da Madeira). EEM is responsible for the electricity supply in the autonomous region, [1].

A simplified grid of the Madeira island grid was

developed for the simulations like explained in chapter 3.

2.2. Scenario definition

It was considered three scenarios:

- **Current scenario:**

Percentage of vRES (wind and solar): $\approx 36\%$

Percentage of renewable (wind, solar and hydro): $\approx 68\%$

Therefore, the nominal power and the power supplied by each power plant for this scenario are shown in table 1.

Table 1: Nominal and supplied power of each power plant for the current scenario.

	Thermal	Hydro	Solar	Wind
Nominal power (MW)	213	77	20	63
Power being supplied before disturbance (MW)	74	77	20	63

- **Future scenario**

Percentage of vRES (wind and solar): $\approx 57\%$

Percentage of renewable (wind, solar and hydro): $\approx 90\%$

The future scenario corresponds to a scenario with an increase in percentage of power provided by solar generation.

Considering that an increase in the nominal power provided by solar generation was undertaken, it was decreased the nominal power of the thermal power plant.

In conclusion, the nominal power and the power supplied by each power plant for this scenario are shown in table 2.

Table 2: Nominal and supplied power of each power plant for the current scenario.

	Thermal	Hydro	Solar	Wind
Nominal power (MW)	100	77	70	63
Power being supplied before disturbance (MW)	24	77	70	63

- **Future scenario with BESS**

Percentage of vRES (wind and solar): $\approx 57\%$

Percentage of renewable (wind, solar and hydro): $\approx 90\%$

The third scenario has the same nominal and supplied power values for each power plant as the future scenario. However, a 15 MW/10 MWh BESS is added like it is planned to happen in the Madeira island power system in the future.

2.3. Disturbances

With the system in steady-state, the following disturbances were undertaken: load step increase (+6 MW, +8 MW, +10 MW), solar generation loss, and ground fault. Then, the values of max frequency deviation, Rate of Change of Frequency (ROCOF) (according to equation 1) and time necessary to reach a steady state were analyzed to understand the frequency stability in each scenario.

$$\text{ROCOF}(t) = \frac{f(t) - f(t - \Delta t)}{\Delta t}, \Delta t = 0.5 \text{ s} \quad (1)$$

3. System Modeling

3.1. Grid

The grid used in the simulations is represented in figure 1.

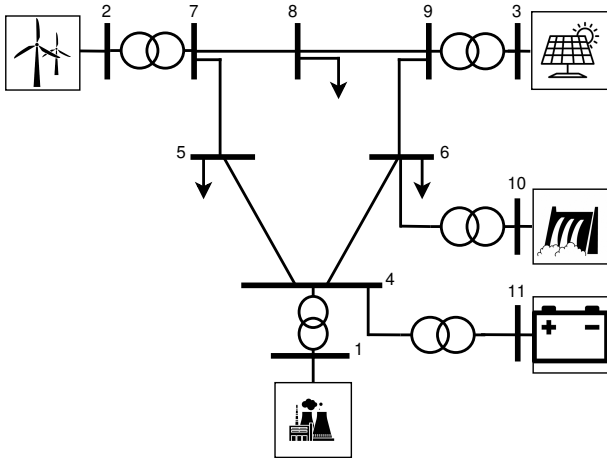


Figure 1: Diagram of the full grid.

For the future scenario without a BESS, the model is the same except for the fact that there is no BESS system connected to bus 4. In the current scenario, besides not having a BESS system, the PV Farm has a lower nominal power (20 MW) as explained in section 3.2 and the thermal power plant has a higher nominal power (213 MW).

3.2. Solar power plant

The solar power station was modeled in a multi-string inverter system configuration as shown in figure 2 based on the model presented in [2].

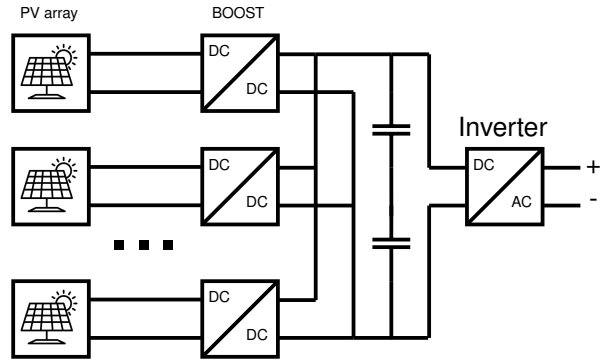


Figure 2: Solar power plant model.

Each PV array + Boost provides an active power of 10 MW in its maximum power point. Therefore, in the current scenario, the PV farm is constituted of 2x PVarray+Boost groups. On the other hand, in the case of the future scenario, it was necessary to use 7x groups of PV array+Boost. At the input of the inverter, there are two capacitors to ensure that the DC voltage is stable and to minimize the oscillations.

The PV arrays are modeled by the *PV Array* block of the Simscape Electrical package that represent an array of photovoltaic modules. Each module is composed of several photovoltaic cells connected in series.

Each PV module is modelled with the five-parameter and 1 diode model represented in figure 3.

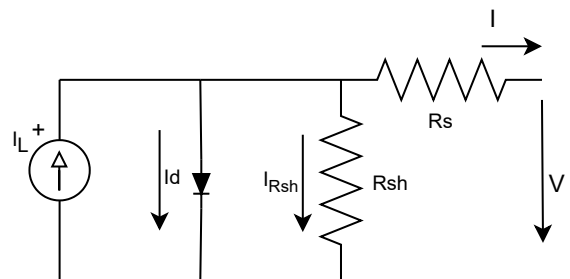


Figure 3: Five-parameter and 1 diode model equivalent circuit.

I_L represents the light-generated current source, R_S the series resistance and R_{sh} the shunt resistance. I_d the diode current (A).

To represent the Boost converter, an average

model from the example in [2] was used. The average model represents the Boost converter by equivalent voltage sources generating the voltage averaged over one cycle of the switching frequency. This model allows using much larger time steps than the detailed model, resulting in a much faster simulation.

The power transfer efficiency from the solar array depends on the sunlight, temperature and load.

These conditions vary; therefore, the relation between the output voltage and current that gives the best power output also changes. The system works at its maximum power point when the relation between the output voltage and current changes to keep power transfer at the highest efficiency.

Therefore it is essential to use a maximum power point tracking (MPPT) to ensure that the PV is always working at the maximum power point. This model uses a MPPT with the "Perturb and Observe" technique.

The inverter was modeled by the *Universal Bridge* block of the Simscape Electrical package. Like with the boost converter, the inverter was also modeled using the average model that represents the Voltage Source Converter (VSC) inverter by equivalent voltage sources. These equivalent voltage sources generate the AC voltage averaged over one cycle of the switching frequency, making the simulations faster than with the detailed model.

The controller for this inverter is based on the controller present in [3] and it is shown in figure 4. Its main goal is to calculate a reference voltage to control the inverter considering the three-phase voltage and current at the solar power plant transformer output. The control ensures that the inverter DC voltage is constant and the reactive power provided at the output is equal to the reference value established. For the simulations performed, the reactive power reference was considered 0.

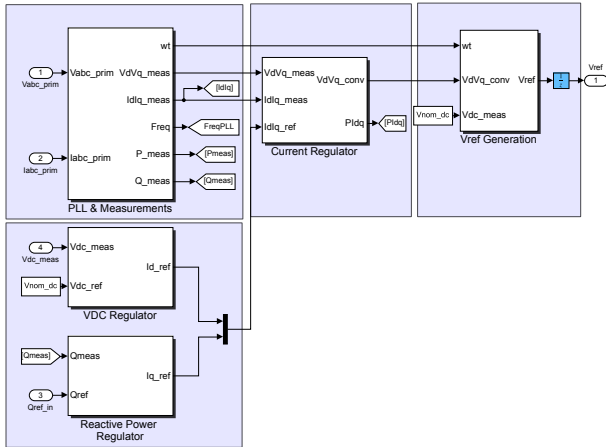


Figure 4: Model of the PV inverter control.

3.3. Wind power plant

The wind power plant model is based in the Simscape model present in the website [4] and in the article [5]. The wind power plant has 42 wind turbines. Each wind turbine has an output power of 1.5 MW and an output voltage of 575 V. The nominal wind speed is 13 m/s.

The model of each wind turbine is represented in figure 5.

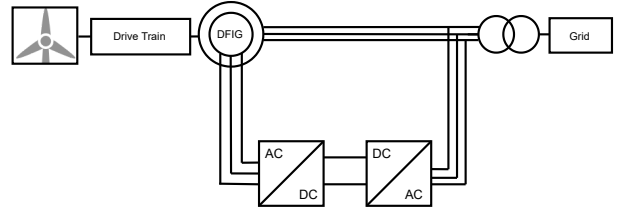


Figure 5: Wind Turbine model.

The doubly fed induction generator (DFIG) was modeled by the *Asynchronous Machine* block of the Simscape Electrical package.

To ensure that the DFIG works at maximum efficiency and that the greatest possible percentage of power is obtained from the wind it is necessary to connect an AC-DC-AC converter to the rotor. This converter allows to change the rotor speed by transferring power through the machine rotor. The power transferred through the rotor by the AC-DC-AC converter is controlled by the wind turbine control. In other words, the wind turbine control, controls the rotor velocity in order to maximize the efficiency of the wind turbine.

When the output power reaches the rated power, the AC/DC/AC system stops maximizing the C_p and works to keep the total power drawn by the stator+rotor constant and equal to the rated power. The rotor blades pitch control (explained below) complements this system to help maintain the system working in rated power.

3.4. Battery energy storage system

The BESS modelled in Simscape Electrical is shown in figure 6.

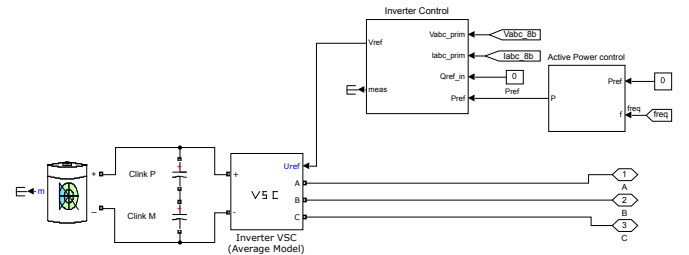


Figure 6: Battery energy storage system model.

The battery was modeled by the *Battery* block of the Simscape Electrical package. For this grid, it was considered a battery with 15 MW power and a storage capability of 10 MWh.

This block implements a generic dynamic model of a lithium-ion battery according to the equivalent circuit represented in figure 7.

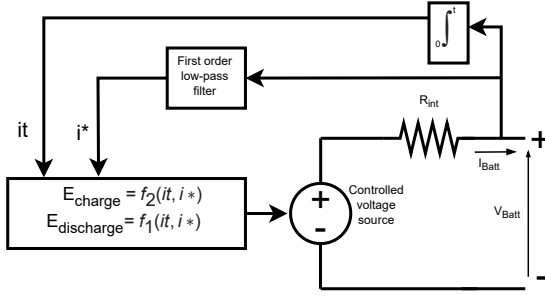


Figure 7: Lithium-ion battery model equivalent circuit.

Being R_{int} the internal resistance, i^* the low-frequency current dynamics and it is the extracted capacity. I_{Batt} and V_{Batt} are the current and voltage at the battery output, respectively.

The inverter is a VSC and the model is the same as the one used in the PV power plant.

The inverter controller used for this inverter is very similar to the one used in the PV power plant. However, in this case, the reference active current (I_d) depends on the imposed output active power (reference active power). The inverter DC voltage can change and the active output power is controlled to be as close to the reference active power as possible

The active power reference is calculated with the active power control block, which will be explained in more detail below. The goal is for the BESS inverter to change its active power output to stabilize the frequency.

Active power control

The active power control implemented resorts to both fast frequency response and synthetic inertia, as shown in figure 8. The upper branch that depends on the difference between the measured frequency and the reference frequency (50 Hz) corresponds to fast frequency response. The lower branch that depends on the frequency derivative corresponds to synthetic inertia.

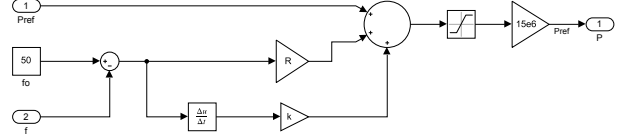


Figure 8: Active power control block implemented in Simscape electrical.

3.5. Thermal power plant

The thermal power plant modeled in Simscape Electrical is represented in figure 9.

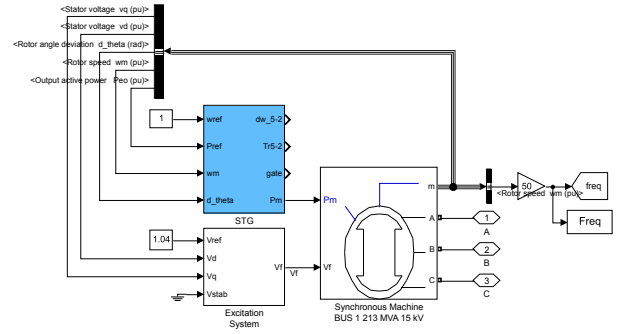


Figure 9: Thermal power plant model.

This power plant works as a swing bus providing the electric power necessary to balance the difference between the power generated and the power requested by the loads.

To model the synchronous generator (SG) mechanical and electrical behaviour it was used the *Synchronous Machine pu Fundamental* block of the Simscape Electrical package.

Electrical model

The dynamics of the stator, field and damper windings are contemplated in this model. The equivalent circuit is represented in figure 10.

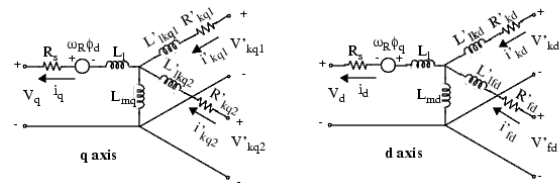


Figure 10: SG equivalent circuit.

Being:

- R : resistance
- ϕ : flux
- L : inductance
- V : voltage
- i : current
- ω : angular frequency

And the subscripts refer to:
d,q : d- and q- axis quantity
R, s : rotor and stator quantity
l,m : Leakage and magnetizing inductance
f,k : Field and damper winding quantity

It is essential to notice that R refers to resistance, but if it is in subscript, it refers to the rotor.

Mechanical model

The mechanical model of the SG is described by equations 2 and 3 used by Simscape electrical SG block.

$$\Delta\omega_r(t) = \frac{1}{2H} \int_0^t (T_m - T_e) dt \quad (2)$$

$$\omega_r(t) = \Delta\omega_r(t) + \omega_{r0}. \quad (3)$$

Being ω_{r0} the rated rotor speed, $\Delta\omega_r(t)$ is the speed deviation with respect to the rated speed of operation at time t, H is the inertia constant, T_e is the electrical torque and T_m is the mechanical torque.

There is two additional blocks from the Simscape Electrical package that allow to control the SG behaviour: the *Steam Turbine and Governor* block and the *Excitation System* block.

3.6. Hydroelectric power plant

The Hydroelectric power plant modeled in Simscape Electrical is represented in figure 11

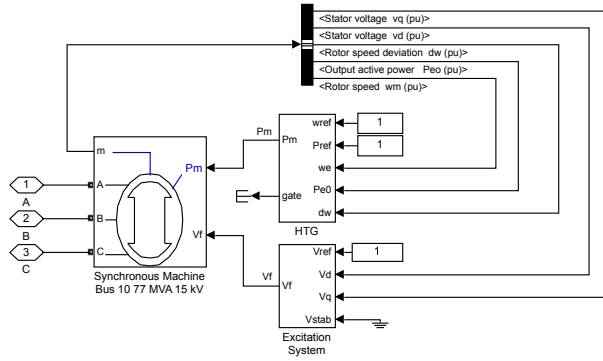


Figure 11: Hydroelectric power plant model.

The hydroelectric power plant is composed by the SG that is identical to the one used in the thermal power plant but with a rated power of 77 MVA and by the controllers.

Like in the thermal power plant there is two additional blocks from the Simscape Electrical package that allow to control the SG behaviour: the *Hydraulic Turbine and Governor block*, and the *Excitation System* block.

3.7. Grid total Inertia

The frequency of the system is a characteristic of the system. Therefore, all the power units can be aggregated into one unit, represented by a single mass model like in [6]. Therefore, the system inertia, H_{sys} , can be obtained by considering the amount of inertia each element of the system provides in relation to its percentage of the total system's power, equation 5.

$$S_{n_{sys}} = \sum_{\forall i} S_{n_i} \quad (4)$$

$$H_{sys} = \frac{\sum_{\forall i} H_i S_{n_i}}{S_{n_{sys}}} \quad (5)$$

Being S_{n_i} the i^{th} generator rated power, H_i its inertia and $S_{n_{sys}}$ the total power capacity of the power system.

Considering the system inertia and the imbalance between the total load and generation power the equation 6 is obtained.

$$\frac{2H_{sys}S_{n_{sys}}}{f_0} \frac{df}{dt} = P_g - P_l \quad (6)$$

Being f_0 the nominal frequency, f the frequency of the system, P_g the total power being generated and P_l the power being consumed.

4. Results

4.1. Load step increase

Current scenario

Three load step increases with different amplitudes, +6 MW, +8 MW and +10 MW, were made in the load connected to bus 6 at time t=1 seg (considering that in t=0 seg, the system is in steady-state). The results for the frequency and ROCOF variation are shown in figure 12 and 13. It is possible to see that an increase in the load demand results in a decrease in the frequency as predicted according to equation 6. It is also visible that a bigger load increase results in a smaller minimal frequency. Furthermore, the ROCOF reaches bigger absolute values for bigger load changes like it was predicted theoretically. According to equation 6, the greater the difference between the generated power and the load demand, the greater the derivative of frequency (ROCOF).

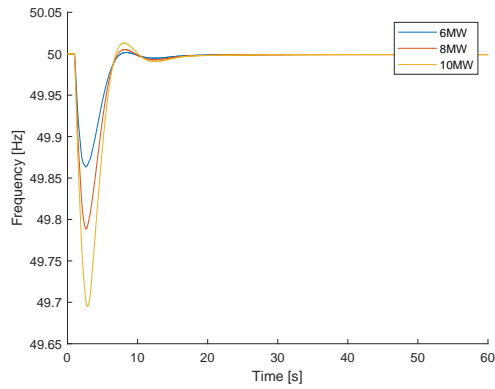


Figure 12: Frequency variation for a load step increase of 6MW, 8MW and 10MW in current scenario.

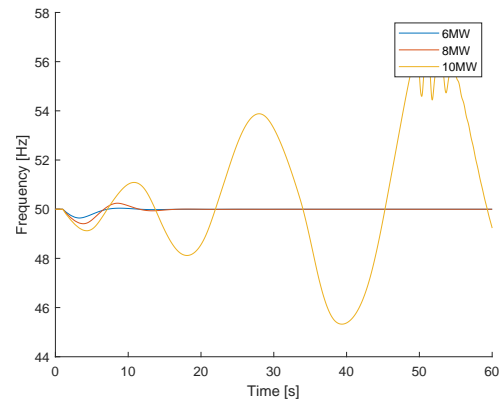


Figure 14: Frequency variation for a load step increase of 6MW, 8MW and 10MW in future scenario.

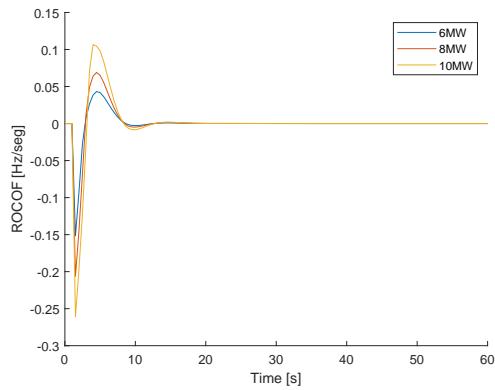


Figure 13: ROCOF variation for a load step increase of 6MW, 8MW and 10MW in current scenario.

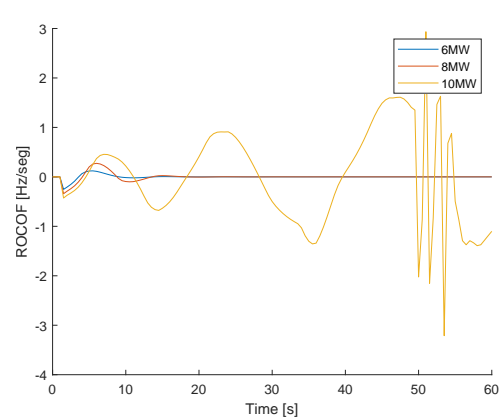


Figure 15: ROCOF variation for a load step increase of 6MW, 8MW and 10MW in future scenario.

Future scenario

The same load step increase was made for future scenario and results are shown in figures 14 and 15. By observing the figure 14 it is visible that the frequency reached such low values for the +10 MW load increase that the SG desynchronized and the system collapsed. The system collapse can be explained by the fact that in the future scenario, the conventional thermoelectric power plant provides less nominal power and more power comes from the solar power plant that does not provide inertia. Therefore, the system is less capable of resisting to bigger disturbances. Once more, it is also possible to verify that a bigger load increase results in a smaller minimal frequency and a more considerable absolute value of ROCOF.

Future scenario with BESS

When applying a load step increase in the future scenario with BESS the results are the ones shown in 16 and 17. When adding a BESS to the future scenario, it is evident that the frequency does not reach such low values as in the current scenario and future scenario without BESS. Furthermore, the frequency goes back to a steady state even for the more considerable load increase of 10 MW. This means a huge increase in the frequency stability as the system did not collapse as it did for the 10 MW load increase in the future scenario without BESS. The frequency is more stable with the use of the BESS because the BESS is faster to react than the thermal power plant.

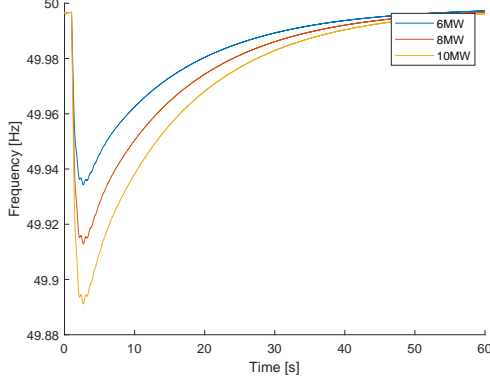


Figure 16: Frequency variation for a load step increase of 6MW, 8MW and 10MW in future scenario with BESS.

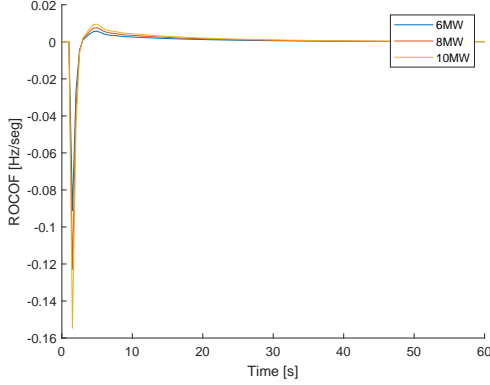


Figure 17: ROCOF variation for a load step increase of 6MW, 8MW and 10MW in future scenario with BESS.

Furthermore, it is also interesting to analyze the BESS energy consumption to maintain the frequency stable. When there is a load step increase of 10 MW (worst case), the BESS system spends only 0.035 MWh to bring the system back to a steady state. Considering that the simulation BESS has a storage capability of 10 MWh, it only spends 0.35% of its capacity to help increase the frequency stability. Table 3 shows the results for minimum frequency reached, the maximum absolute value of ROCOF and time to reach a steady state after the disturbance for the load step increase disturbance in all scenarios. When analyzing the 10 MW load increase, the benefits of the BESS are evident as the system collapsed for the future scenario without BESS and with the addition of the BESS, the system was able to go back to steady state 52.10 seg after the disturbance.

Table 3: Results of load step increase for all scenarios.

scenarios	(current)/(future)/(future+BESS) scenarios		
	Min frequency (Hz)	Max absolute value of ROCOF (Hz/s)	Time to reach steady state again (s)
6 MW	49.86/49.64/ 49.93	0.15/0.25/ 0.09	12.38/15.56/ 43.63
8 MW	49.79/ 49.41/ 49.91	0.21/0.34/ 0.12	13.75/21.98/ 48.32
10 MW	49.69/56.59/ 49.89	0.26/3.21/ 0.15	14.49/ doesn't reach /52.10

4.2. Generation loss

For the generation loss disturbance, a 50% decrease in the irradiation that hits the solar panels (from 1000 W/m^2 to 500 W/m^2) was analyzed. This translates in a 50% decrease (-35 MW) in the PV power supplied in the future scenario with and without BESS. For the current scenario, a 50% decrease in the irradiance means a -10 MW decrease in the power. The effect this disturbance has in the frequency and in the ROCOF is shown in figures 18 and 19.

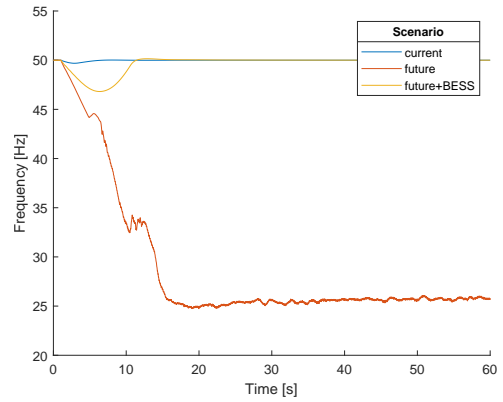


Figure 18: Frequency variation for a generation loss of (-50%) in the current (-10 MW), future (-35 MW) and future with BESS scenario (-35 MW).

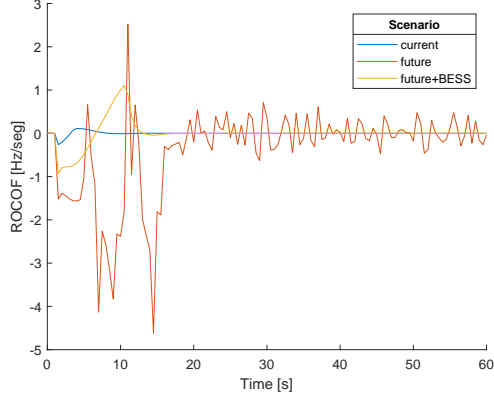


Figure 19: ROCOF variation for a generation loss of (-50%) in the current (-10 MW), future (-35 MW) and future with BESS scenario (-35 MW).

The generated power decreased and the load demand stayed constant. Therefore, according to equation 6 the frequency has a negative variation, as it can be confirmed experimentally in figures 18 and 19. In the future scenario without BESS, the SG desynchronized and the system collapsed. However, when adding a BESS, the system could go back to a steady state, but not before reaching a minimal frequency of 46.81 Hz, which would undoubtedly cause problems in the grid. The grid's frequency cannot reach such values because that would affect the work of industrial machines that depend on the grid frequency to be near 50 Hz.

Table 4 shows the results for minimum frequency, maximum absolute ROCOF and time to reach steady state for all scenarios in the case of a generation loss of 50%.

Table 4: Results of a -50% solar generation loss for all scenarios.

scenarios	-50% solar generation loss		
	Min frequency (Hz)	Max absolute value of ROCOF (Hz/s)	Time to reach steady state again (s)
current	49.69	0.26	14.49
future	24.74	4.62	doesn't reach
future+BESS	46.81	1.10	34.53

4.3. Ground Fault

The third type of disturbance simulated was a three-phase ground fault in bus 5 at $t=1$ seg. By imposing a 200 ms short circuit in bus 5 the 72.5 MW/10 Mvar load that is connected to that bus gets short circuited. The effect on the frequency and ROCOF of this disturbance is shown in figures 20 and 21. Once more, the system could not go

back to a steady state in the future scenario without BESS. On the other hand, the system could go back to steady-state 27.36 seg after the disturbance in the future scenario with BESS. The results for the 200 ms ground fault in bus 5 for all scenarios are summarized in table 5.

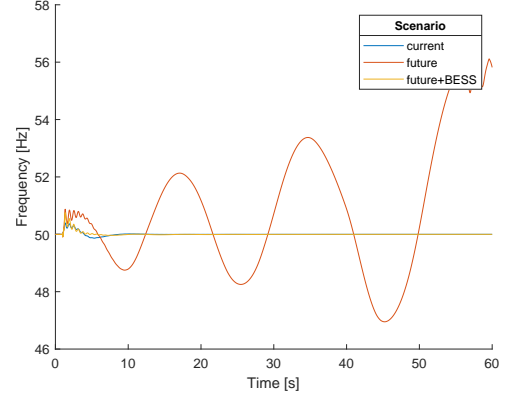


Figure 20: Frequency variation for a 200 ms ground fault in bus 5 in the current, future and future with BESS scenario.

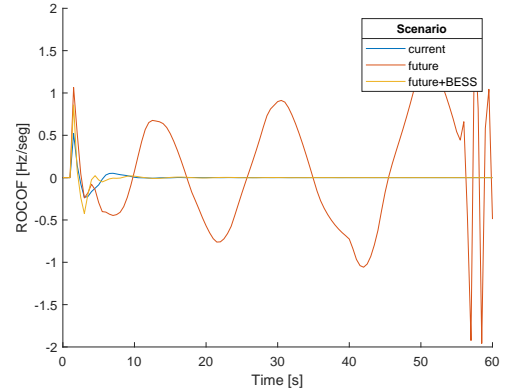


Figure 21: ROCOF variation for a 200 ms ground fault in bus 5 in the current, future and future with BESS scenario.

Table 5: Results of a 200 ms ground fault for all scenarios.

scenarios	200 ms ground fault in bus 5		
	Max frequency (Hz)	Max absolute value of ROCOF (Hz/s)	Time to reach steady state again (s)
current	50.40	0.52	11.22
future	56.25	1.96	doesn't reach
future+BESS	50.76	0.86	27.36

5. Conclusions

In the current scenario, the system reacted well to the disturbances, always returning to a steady state after a short time period and not reaching very low values of frequency. On the other side, when the percentage of solar generation increased from 8.5% (35.5% of vRES), current scenario, to 30% (56.8% of vRES), future scenario, the system started to collapse when certain disturbances were applied. This leads to conclude that as the PV integration increases, it also increases the grid's susceptibility to irradiation and load changes, increasing the frequency instability. Afterward, a BESS was added to the future scenario and the same generation/load step change and ground fault simulations were performed. It was concluded that after a load step change of 6 MW, 8 MW and 10 MW, the system could always return to a steady state. By adding a BESS, the system could also go back to a steady state after a 50% generation loss as opposed to the case without BESS. However, in this case, the frequency stability is still better in the current scenario because a 50% generation loss in the current scenario means a 10 MW loss, and in the future scenario, a 50% generation loss represents a -35 MW change in the generation. The ground fault was the disturbance that caused more instability in the frequency. But once more, the BESS allowed the system to go back to a steady state which didn't happen for the future scenario without BESS where the SGs desynchronized. It is important to highlight that for the BESS to improve the frequency stability significantly, it is essential to have considerable power to respond to fast load and generation changes. In conclusion, according to the results obtained, it is confirmed that an increase in the PV integration results in an increase in the system's vulnerability to disturbances. More specifically, it negatively impacts the frequency stability, leading to the system collapse when a significant disturbance occurs. These simulation results are explained by the decrease in the inertia that the thermoelectric power plants provide. Furthermore, these results endorse the positive effect that a BESS with a suitable control mechanism has in increasing the frequency stability. In some instances, it was even proved that the BESS could avoid the system collapse. Therefore, the installation of BESS in weak grids can be a strong ally in increasing renewable sources penetration and reaching the goal of net zero.

5.1. Future Work

Several improvements can be made to this work to prove the positive impact of storage systems on the

frequency stability of weak grids. First, it could be tested using different storage systems like pumping, supercapacitors, or fuel cells. Furthermore, a more accurate model of the Madeira grid could be used to test the performance of the BESS in a system closer to reality. In a future study, it could also be tested a system with no conventional generation and the use of a BESS system with bigger power and capacity as the swing bus.

References

- [1] DEP – Direção de Estudos e Planeamento. CARACTERIZAÇÃO DA REDE DE TRANSPORTE E DISTRIBUIÇÃO EM AT E MT. Technical report, DEP – Direção de Estudos e Planeamento, 3 2022.
- [2] Mathworks example of a 400 kW grid connected PV farm.
- [3] MathWorks example of a 2 MW PV farm.
- [4] Richard Gagnon. Wind farm - DFIG average model.
- [5] Nicholas W Miller, Juan J Sanchez-Gasca, William W Price, and Robert W Delmerico. Dynamic modeling of ge 1.5 and 3.6 mw wind turbine-generators for stability simulations. In *2003 IEEE Power Engineering Society General Meeting (IEEE Cat. No. 03CH37491)*, volume 3, pages 1977–1983. IEEE, 2003.
- [6] Pieter Tielens and Dirk Van Hertem. The relevance of inertia in power systems. *Renewable and Sustainable Energy Reviews*, 55:999–1009, 2016.